

Synthesis of Shape Morphing Compliant Mechanisms Using a Load Path Representation Method

Kerr-Jia Lu^{*} and Sridhar Kota

Department of Mechanical Engineering, University of Michigan, Ann Arbor, MI 48109

ABSTRACT

The performance of many mechanical systems is directly related to the geometric shapes of their components, such as aircraft wings and antenna reflectors. While the shapes of these components are mostly fixed, incorporating shape morphing into these systems can increase the flexibility and enhance the performance. A synthesis approach for shape morphing compliant mechanism is presented in this paper, using a load path representation method to efficiently exclude the invalid topologies (disconnected structures) from the Genetic Algorithm (GA) solution space. The synthesis approach is illustrated through a flexible antenna reflector design and a morphing aircraft trailing edge. The results demonstrate the capability of the load path representation method to create various designs with less design variables. The results also show that the use of compliant mechanisms can indeed provide a viable alternative for shape morphing applications. Methods to improve convergence such as employing a local search within or following the GA are also discussed.

Keywords: compliant mechanism, adaptive structure, shape morphing, genetic algorithm, topology optimization

1. INTRODUCTION

The performance of many mechanical systems is directly related to the geometric shapes of their components, such as aircraft wings and antenna reflectors. The wing shape affects the obtained lift and drag, while the antenna reflector shape determines the signal radiation pattern. The concept of 'shape morphing' in these systems have been studied extensively to improve system functionality and flexibility. In this paper, we use antenna systems to illustrate the synthesis of shape morphing compliant mechanisms.

The typical lifetime for a satellite can exceed 15 years while the per vendor useful life of a particular antenna on that satellite can be as little as five years¹. To fully utilize the antenna, an optimal situation is to sell the antenna to another vendor. However, the new vendor might require service over a geographical region or signal pattern that is different from the original one. Two traditional methods for generating contoured radiation patterns include array antennas and shaped/contoured reflector systems. An array antenna is an aggregation of radiating elements in an electrical and geometrical arrangement, which will result in the desired radiation characteristics that may not be achievable by a single element. It generates appropriate signal pattern by selective excitation of current distribution of each element. Although the array antenna can change its signal pattern by controlling the excitation current, it generally has higher cost, heavier weight, and lower efficiency (due to heat dissipation). On the other hand, a contoured reflector antenna produces a radiation pattern with a specific reflector shape. Although this type of antenna is low cost and versatile, it usually has a fixed shape and can only generate one radiation pattern. Therefore, various mechanically reconfigurable or shape changing reflector antennas have been developed to enhance the system flexibility required in different tasks.

The majority of research on shape changing reflectors involves the use of rigid-link assemblies and the use of smart material actuators. Antenna reflectors using rigid-links typically consist of discrete rigid panels that are hinged together². The reflector shapes can be changed by controlling the relative angles at the hinges between multiple panels. Although the piecewise hinged antenna reflector can be reconfigured into various shapes, it may require a relatively complicated control scheme for a system with so many degrees of freedom. In addition, the hinges generate discontinuity on the reflector surface and the associated backlash errors may reduce the system accuracy. On the other

^{*} kjlu@umich.edu; phone 1 734 763 4916; Department of Mechanical Engineering, University of Michigan, 2250 G.G.Brown, 2350 Hayward, Ann Arbor, MI, 48109-2125, USA

hand, antenna reflectors incorporating smart materials have smoother surfaces and fewer actuators^{1,3,4,5,6,7,8}. However, the actuators only provide a small displacement output that might not scale up proportionally for larger reflectors. An alternative solution is to use a shape morphing compliant mechanism to achieve the desired shape morphing with the structural deformation induced by an input actuation. It provides a novel means for shape morphing with better scalability and simpler control scheme.

We previously developed an approach to systematically synthesize shape morphing compliant mechanisms^{9,10}. The synthesis approach incorporates a Genetic Algorithm (GA) to search for the optimal topology and dimensions for the compliant mechanisms. However, the design variable definition, inevitably, includes many infeasible topologies (disconnected structures) in the design space, and, in turn, makes the GA search inefficient. In this research, we developed a load path representation method to ensure all designs are feasible and exclude the invalid designs from the solution space. A brief introduction to compliant mechanism design will be given in the next section, including the previously developed shape morphing compliant mechanism synthesis approach, followed by the load path representation method developed in this research. For more details regarding the overall synthesis approach, interested readers should refer to earlier papers by the authors^{9,10}.

2. BACKGROUND: INTRODUCTION TO COMPLIANT MECHANISM DESIGN

A compliant mechanism is a single-piece flexible structure where the structural deformation is used to provide a motion or force output with an input actuation. It works as a transmission that is designed to have the desirable characteristics between the input actuation and the output to the environment. Typical compliant mechanism synthesis involves the use of homogenization method^{11,12} or truss/beam grounded structures^{9,13,14,15}, originally seen in structural optimization. These methods can be incorporated with different objective functions to design compliant mechanisms for various purposes, such as compliant grippers for object manipulation¹⁵, compliant motion amplifier in MEMS¹⁴, and compliant end-effector for minimally invasive surgery¹⁶. However, very little attention has been directed to adaptive shape morphing problems. Saggere and Kota¹⁷ first proposed a synthesis method to demonstrate the use of compliant mechanisms for shape morphing. Although the results show that the approach is viable for real-scale practical applications, the structural topology generation still requires input based on intuition or design experience. In order to make the synthesis process more systematic, we previously developed a synthesis approach that incorporates a Genetic Algorithm (GA) to simultaneously determine the topology and dimensions for the shape morphing compliant mechanisms^{9,10}. The flowchart of the approach is shown in Figure 1.

There are three major components in the synthesis approach shown in Figure 1: (1) the GA to search for the optimal compliant mechanism, (2) the Finite Element Analysis (FEA) to solve for the structural deformation, and (3) the curve comparison schemes to evaluate the performance of each design in GA. Assuming the shape change is mainly obtained from bending of the structure (beams), the approach starts with examining the curvature difference between the initial and target curve profiles to determine if the shape morphing is attainable. From linear beam theory, the bending stress is proportional to the curvature after bending. Therefore, the stress can be estimated from the curvature difference to check against failure. The design domain is then parameterized in terms of the design variables, including the topology, size, and shape variables of the compliant mechanism. The GA, then, starts the search by randomly generating an initial population of designs and creating successive new generations from reproduction of the first one. The reproduction scheme involves a selection scheme, followed by crossover and mutation operations. A curve comparison scheme is used to evaluate 'shape deviation' of new designs created from the genetic operations. The shape deviation provides a criterion to rank the performance of each design in a generation, in order to facilitate the selection process into the next generation. This reproduction repeats until reaching a pre-specified maximum number of generations, and the optimal compliant mechanism design can be obtained.

The results in the previous studies^{9,10} have shown that the shape change can indeed be achieved using the compliant mechanism obtained from the synthesis approach. However, the design domain parameterization (shown bold in Figure 1), in fact, allows the generation of invalid structures that are topologically disconnected. Figure 2 shows an example of the initial discretization network and the three types of invalid structures that can be generated using this parameterization scheme. Although these invalid designs can be detected and penalized in GA, this makes the search

inefficient. In this research, we developed a parameterization method that utilizes a load path representation scheme to ensure all designs are valid.

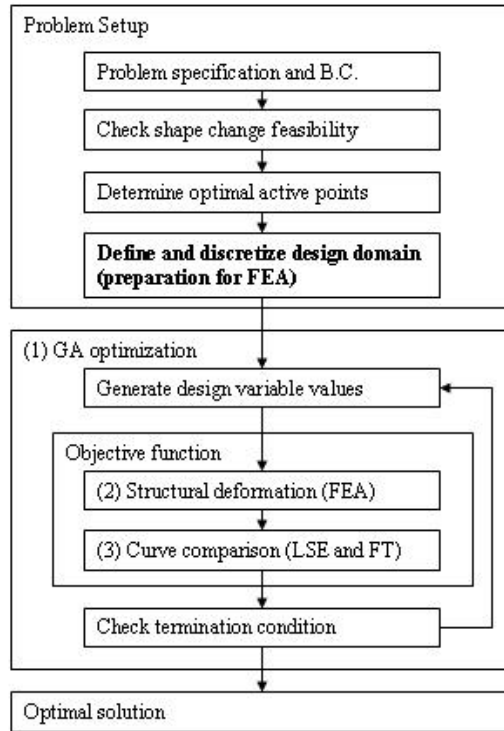


Figure 1: Flowchart of the compliant mechanism synthesis approach for shape morphing.

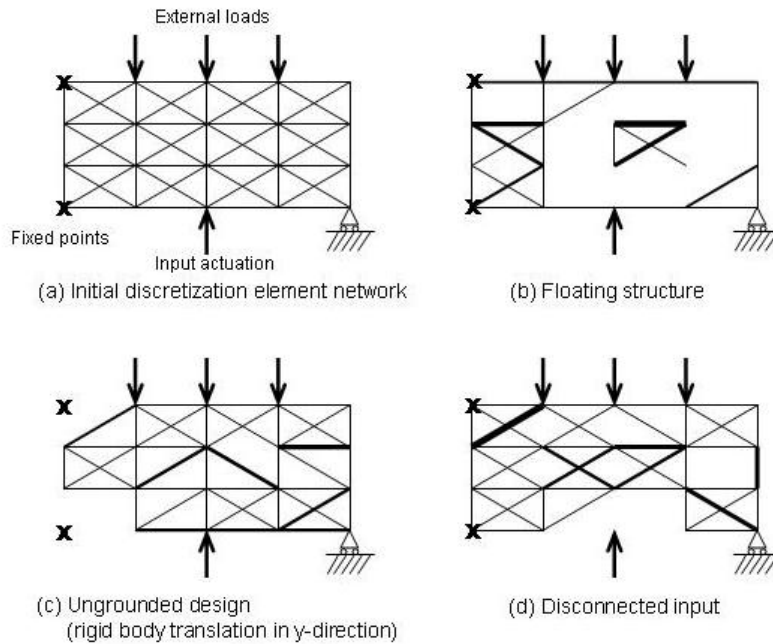


Figure 2: (a): the initial design domain discretization using a beam element network. Each element is described by a binary topology variable (h_{Top}) and a continuous dimensional variable (h_{Dim}), while the resulting beam dimensions are $h = h_{Top} \times h_{Dim}$. (b)-(d): Three types of invalid structures that can be generated from (a) when some h_{Top} values are set to zero.

3. METHODOLOGY

In order to ensure the validity of all designs generated in GA, we developed a design domain parameterization method that utilizes the load path of a structure. A typical compliant mechanism problem involves three components: an input point, one or more output points, and at least one fixed point. These points should be connected either directly or indirectly to each other through the ‘load paths.’ The compliant mechanism topology can, then, be represented with paths connecting these points. As can be seen in Figure 3, the connection generates three types of paths: from input to outputs, from input to fixed points, and from fixed points to output points. However, direct connection between the points limits the attainable topology connectivity. In order to increase the variety of available topologies, a set of grid points are used as the intermediate ‘connection ports’ to allow additional connections between paths. As shown in Figure 4 and Table 1, all paths are now represented as a sequence of nodes, and the intermediate connection between paths can only occur at the connection ports. According to the connectivity of the design, ports 6, 7, and 11 are termed as active connection ports, while ports 8, 9, and 10 are inactive. The use of connection ports not only increases the variety of available topologies, but it also allows the existence of overlapping elements (section 1-6 and 2-7), which can potentially be expanded to generate three-dimensional topologies.

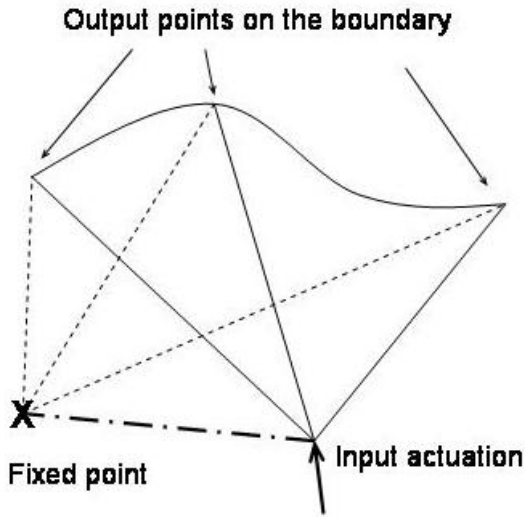


Figure 3: Three types of paths (shown in solid, center, and dash lines respectively) are used to connect the input to output, input to fixed point, and fixed point to output. Note that the generated paths may crossover each others, but there are no connections at the intersection points.

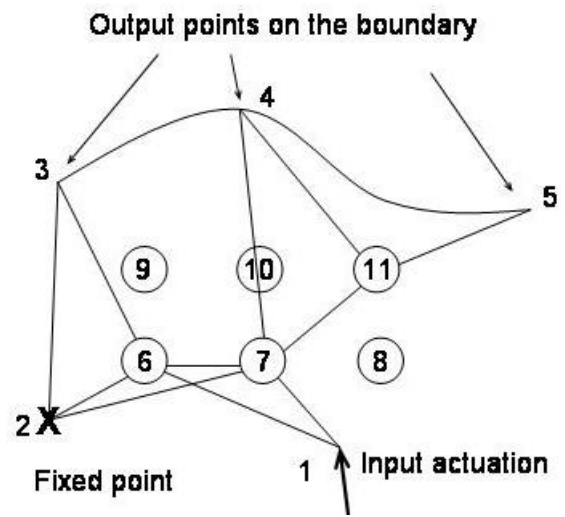


Figure 4: An example topology with 3 active connection ports (6, 7, and 11) and 3 inactive ones (8, 9, and 10). Each path is represented as a sequence of nodes, shown in Table 1. Although the two-dimensional plot of the topology shows an intersection between section 1-6 and 2-7, there is not physical connection between the two paths.

Path #	Start point	End point	Path sequence
1	Input (1)	Output (3)	{1,6,3}
2	Input (1)	Output (4)	{1,7,11,4}
3	Input (1)	Output (5)	{1,7,11,5}
4	Input (1)	Fixed (2)	{1,6,2}
5	Fixed (2)	Output (3)	{2,3}
6	Fixed (2)	Output (3)	{2,6,7,4}
7	Fixed (2)	Output (5)	{2,7,11,5}

Table 1: The path sequences for the topology in Figure 4.

3.1. Topology design variables

Most of the published literatures in structural topology optimization involve the discretization of the design domain into a finite element mesh, using QUAD elements¹² or Truss/Beam grounded structures^{9,13,14,15}. The design variables are typically the material/density variables for QUAD elements or cross-section dimensions for the truss/beam approach. Since each element has a corresponding topology variable, the number of design variables increases as the discretization resolution gets higher. Using the path representation method developed in this research, the number of design variables is independent of the design domain resolution.

In this research, the topology of the compliant mechanism is described by the connecting sequences of the paths and the corresponding binary variable ($pTop_i$) for each path. The binary variable, $pTop_i$, determines the existence ($pTop_i = 1$) or elimination ($pTop_i = 0$) of the i^{th} path. Figure 5 and Figure 6 are two designs that have the same basic topology as the example in Figure 4 with some $pTop_i$ values set to zero. Their corresponding topology information can be found in Table 2. The topology of the compliant mechanism is finally created by connecting these load paths with linear beam elements.

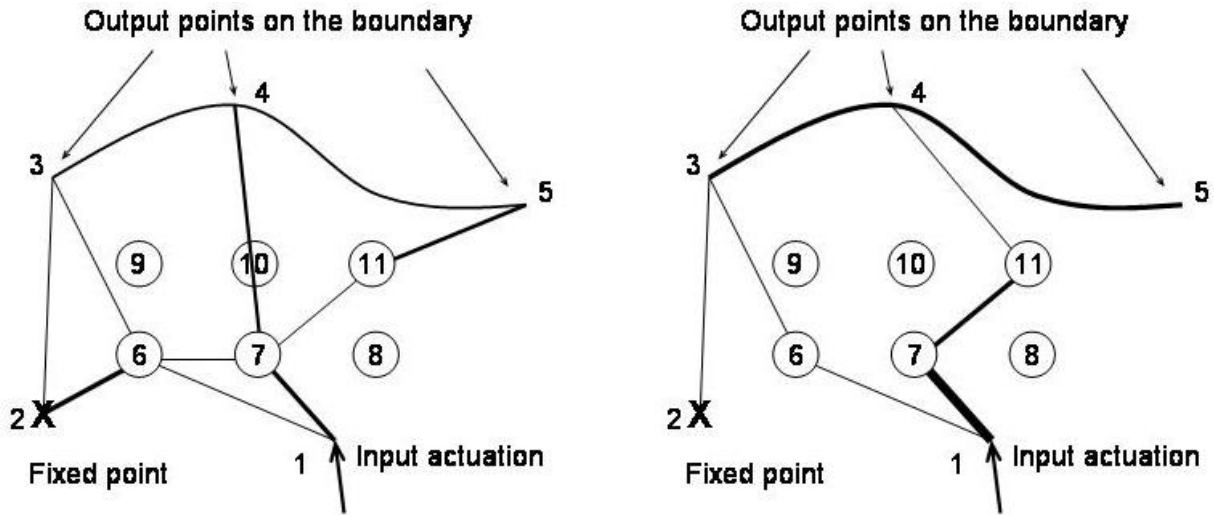


Figure 5: This design has the same connectivity as that in Figure 4, but the topology variables, $pTop_2$ and $pTop_7$, are zeros. The topology and dimensional information for this design can be found in Table 2 and Table 3 respectively.

Figure 6: By changing the $pTop$ values for the design in Figure 4, a different topology can be obtained. Its corresponding topology information is shown in Table 2.

Path #	Path seq.	$pTop_i$ Fig.5	$pTop_i$ Fig.6
1	{1,6,3}	1	1
2	{1,7,11,4}	0	1
3	{1,7,11,5}	1	0
4	{1,6,2}	1	0
5	{2,3}	1	1
6	{2,6,7,4}	1	0
7	{2,7,11,5}	0	0

Table 2: The topology information for the designs shown in Figure 5 and Figure 6.

3.2. Dimensional design variables

The dimensional variables, on the other hand, are the cross-section dimensions of the beam element connecting the paths. In this research, we are assuming linear beam elements with rectangular cross-sections. In addition, the cross-section remains constant between two consecutive connection ports. For a given path, there can be one or more

‘sections,’ depending on the length of the path sequence. A sequence of continuous variable, $pDim_i$, is assigned to each path to describe the in-plane beam dimensions, while the out-of-plane dimension is held fixed. Hence, the $pDim_i$ array is always one element shorter than the path sequence in length. The same example shown in Figure 5 is used to illustrate the definition of dimensional variables with its topology and dimensional information listed in Table 3. As can be seen, each path has a corresponding $pDim_i$ array, but, due to the different $pTop_i$ values, some paths are not shown in the design. Note that some paths have overlapping sections with another path; for example, path #4 and #6 have an overlapping section between port 2 and 6 (shown bold in Table 3). That is, there are two different dimension values for this section, $pDim_4(2) = 1.3$ and $pDim_6(1) = 3$. Since only one value is required to describe the section dimension, one $pDim$ value is randomly selected from the potential values (1.3 and 3 in this case) with uniform probability. The selected value will, then, overwrite the other values.

In addition to the path section dimensions ($pDim_i$), another continuous variable, $hBoundary$, is used to represent the dimension of the boundary. In this research, it is assumed that the shape morphing boundary always exists in every design, and the boundary has a uniform cross-section. Therefore, it is unnecessary to assign a topology variable for the boundary, and only one dimensional variable is used to represent the boundary dimension.

Path #	Path seq.	$pTop_i$	$pDim_i$
1	{1,6,3}	1	{1,0.75}
2	{1,7,11,4}	0	{1,1,2}
3	{1,7,11,5}	1	{3,0.75,2.5}
4	{1, 6 ,2}	1	{2.5, 1.3 }
5	{2,3}	1	{0.75}
6	{ 2 ,6,7,4}	1	{ 3 ,1.5,2.25}
7	{2,7,11,5}	0	{1.8,1,1}

Table 3: The topology and dimensional information for the design shown in Figure 5.

3.3. Shape design variables: connection port locations

As opposed to the fixed FEA mesh approach used in previous research^{9,10}, the path representation of design domain generates a mesh that changes with the locations of the connection ports. This is accomplished by allowing the connection ports to move within a specified region, thus their locations can be regarded as the shape variables. While the connectivity between the connection ports determines the topology of a compliant mechanism, the locations of them determines ‘shape’ of the path. Figure 7 shows a design having the same topology as that in Figure 5. By merely changing the locations of two active connection ports (6 and 7), the two designs now have very different appearances. As can be seen, the two designs have the same connectivity but different section lengths and orientations.

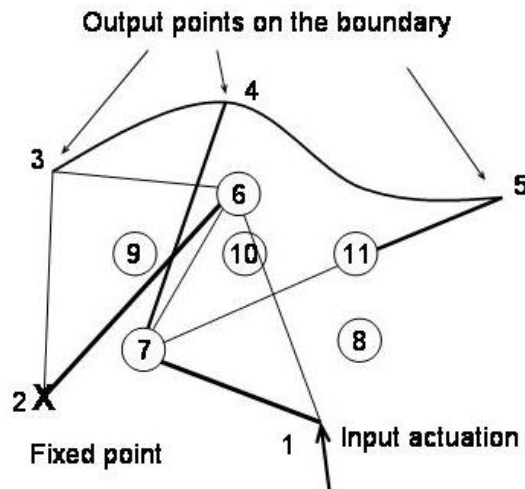


Figure 7: A design having the same topology as that in Figure 5 but different connection port locations (port #6 and #7).

3.4. Constraints

By studying the invalid topologies shown in Figure 2(b)~(d), we found two basic requirements for a design to be valid: (1) the structure needs to be grounded with one or more fixed points, and (2) the input has to be connected to the rest of the structure. These rules can easily be incorporated in the path representation parameterization by monitoring the $pTop_i$ values of paths from input and fixed point to the output points. At least one of the $pTop_i$ values in each path category has to be 1. This is a huge advantage over the grounded structure approach (Figure 2), where a topology variable only determines the existence of ‘one element.’ The connections (paths) between the input/fixed points to the output points are explicitly shown in the $pTop_i$ variables, whereas this connection information has to be ‘searched for’ in the grounded structure approach. In addition to the two validity requirements (constraints), a stress constraint is applied to prevent yielding in the compliant mechanism, and a strength constraint is used as a stiffness requirement for the structure to withstand external loads.

3.5. Objective function: curve comparison

The objective for the optimization is to find the optimal topology and dimensions for the compliant mechanism that can achieve the desired shape change with minimum error. To evaluate the ‘performance’ of each design, we used the Least Square Error (LSE) formulated previously to find the ‘shape deviation’¹⁰. The deviation is measured based on the sampling points on the deformed and target curves illustrated in Figure 8. The target curve is the desired profile after shape morphing, while the deformed curve is what a particular compliant mechanism actually achieves with the input actuation. The LSE deviation is defined in equation (1), using the sampling points on the curves, $P_{TAR,i}$ and $P_{DEF,i}$. The smaller the deviation is, the closer the design can achieve the desired shape morphing. Interested readers should refer to Lu and Kota¹⁰ for more details on the objective function formulation.

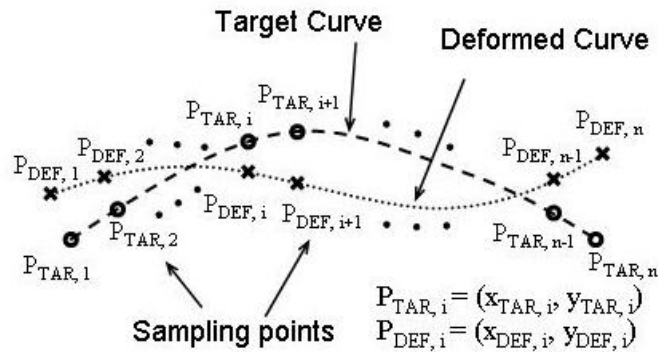


Figure 8: The deformed curve is the compliant mechanism boundary shape after input actuation. The target curve is the desired boundary profile after shape morphing. The curves are sampled by two sets of discrete data points, which are used to evaluate the shape deviation values.

$$LSE_{deviation} = \frac{1}{n} \sum_{i=1}^n \sqrt{(x_{DEF,i} - x_{TAR,i})^2 + (y_{DEF,i} - y_{TAR,i})^2}, \quad (1)$$

where n is the number of sampling points on each curve.

The optimization problem can be summarized in eqn.(2) ~ (11). The objective is to minimize the LSE deviation between the deformed and target boundary profiles. The structural deformation is solved for using a finite element analysis (FEA). The beam element dimensions (in-plane) are constrained between a minimum and maximum values, typically based on the manufacturing constraints. Equation (6) shows the beam dimensions, resulting from the topology and dimensional design variables. A stress constraint in eqn.(7) is imposed on all the elements. The locations of the connection ports are allowed to wander within a specified range, as shown in eqn.(8). The validity requirements, equations (9) and (10), are also included in the constraints to ensure all the generated designs are properly connected. As shown in eqn.(11), the stiffness is achieved by constraining the maximum nodal displacement to stay

within an acceptable value, when the actuator is inactive. The optimization problem is then solved with a genetic algorithm to handle discrete and continuous variables.

Objective Function

$$\min_{pTop_i, pDim_i, hBoundary, portLocation} (LSE_{deviation}) \quad (2)$$

Subject to

$$\mathbf{d} = \mathbf{K}^{-1}\mathbf{F} \quad \begin{array}{l} \text{Equilibrium condition} \\ \text{(Solving for structural deformation from FEA)} \end{array} \quad (3)$$

$$pDim_{min} < pDim_{i,j} \leq pDim_{max} \quad \text{Size constraint for path sections} \quad (4)$$

$$pDim_{min} < hBoundary \leq pDim_{max} \quad \text{Size constraint for boundary curve} \quad (5)$$

$$h_e = pTop_i \times pDim_{i,j} \quad \text{Section in-plane dimension definition} \quad (6)$$

$$\sigma_e \leq \sigma_{allowable} \quad \text{Stress constraint} \quad (7)$$

$$(x_{min}, y_{min}) \leq portLocation \leq (x_{max}, y_{max}) \quad \text{Port location constraint} \quad (8)$$

$$\sum_{i \in pathInOut} pTop_i \geq 1 \quad \text{Structural validity requirement} \quad (9)$$

$$\sum_{i \in pathFixOut} pTop_i \geq 1 \quad \text{Structural validity requirement} \quad (10)$$

$$\max(d_{unactuated}) \leq d_{allowable} \quad \text{Stiffness constraint} \quad (11)$$

where $pTop \in \{0,1\}$; $pDim, hBoundary, portLocation \in \mathbb{R}^+$;
i: path number; *j*: section number in the *i*th path; *e*: number of elements.

3.6. Implementation in genetic algorithm: crossover and mutation

Crossover and mutation are two genetic operations commonly seen in GA. The crossover and mutation strategies determine the varieties of designs that can be generated in the GA process. Typical GA represents the design variables into an array or string, analogous to the genes on the DNA. The crossover is usually done by exchanging one or more segments between two chromosome strings. On the other hand, the mutation is done by altering one randomly selected element on the chromosome string. However, for a more complicated design variable data structure, such as the path representation, the crossover and mutation strategies have to be more sophisticated. We, therefore, developed several simple strategies to work with the path representation parameterization in this research.

With the path representation method, the crossover strategy in this approach is to ‘exchange’ the path sequence, *pTop*, and *pDim* information of several randomly selected paths within two parent designs. This process produces new topology connectivity and changes the section dimensions at the same time. With the new path sequence info, new active/inactive connection ports can be generated. When a new active connection port is generated, a new port location is randomly selected within the design domain. In addition, the boundary dimension (*hBoundary*) of the two parent designs can be exchanged according to the crossover probability.

For the mutation process, the boundary dimension is replaced by a randomly generated value within the upper and lower bounds. In addition, the destinations (end points) of some randomly selected paths can mutate to a different one within

the same category. For example, a path originally connecting the input to one of the output points can be mutated into a path connecting the input to another output point, simply by changing the last component in the path sequence.

4. DESIGN EXAMPLES

Flexible antennas and morphing aircrafts are two potential areas where shape morphing can enhance the system performance and increase flexibility. A flexible antenna reflector and a morphing aircraft trailing edge are shown in this section to illustrate this synthesis approach.

4.1. Antenna reflector beam steering

Figure 9 is an example of antenna reflector in its beam-steering mode that changes the orientation of the reflector, and in turn, varies the coverage area. In this example, we design a compliant mechanism that is capable of simulating a rigid body rotation about the center. The GA starts with an initial population of 100 individuals and allows 80 generations, while the crossover and mutation probabilities are 0.8 and 0.3 respectively. As shown in Figure 9, the shape morphing is achieved with an input of 2mm in the negative x-direction, while the top boundary is subjected to a constant load of 1N downwards. The resulting LSE deviation is 0.9964mm with a maximum stress of 19.9MPa ($< 34.45\text{MPa}$, the yielding stress for ABS). The minimum and maximum in-plane beam dimensions are 1.88mm and 2.98mm respectively, and the out-of-plane dimension is 4mm in this design.

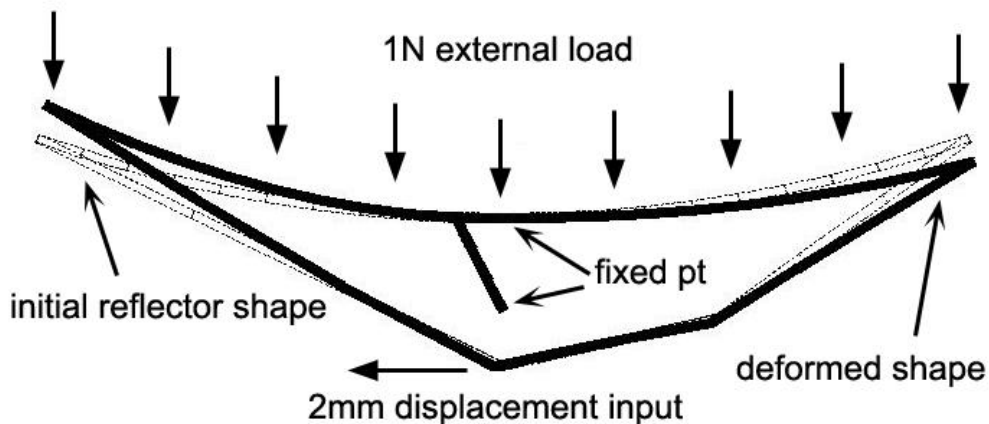


Figure 9: Two ends of the antenna reflector are required to bend upwards and downwards to simulate a change in orientation of 3° clockwise. The horizontal dimension of this antenna model is 200mm, and the vertical dimension is 30mm. Maximum deflection is 7.514mm upwards at the left tip. The minimum and maximum in-plane beam dimensions are 1.88mm and 2.98mm, while the out-of-plane dimension is 4mm.

4.2. Aircraft trailing edge shape morphing

Most aircraft wings are optimized to produce minimum drag under a particular flying speed, at which the largest proportion of fuel is expended. However, in reality, flying speed varies continuously throughout flight. Hence, to obtain optimal fuel efficiency, the wing shape should be able to change in response to the change in flying speed⁹. As shown in Figure 10, we design a compliant trailing edge that is able to deflect 10 degrees downwards to enhance the handling and maneuvering capabilities. The GA starts with an initial population of 80 and allows 80 generations, while the crossover and mutation probabilities are 0.8 and 0.3 respectively. The shape morphing is achieved with an input of 2inch displacement at an angle of -11.4287 degrees without any external load. The resulting LSE deviation is 0.50217inch, while the maximum stress is 32989psi ($< 33000\text{psi}$, the yielding stress for aluminum). In addition, the minimum and maximum in-plane beam dimensions are 0.052inch and 0.1174inch respectively, and the out-of-plane dimension is 1 inch.

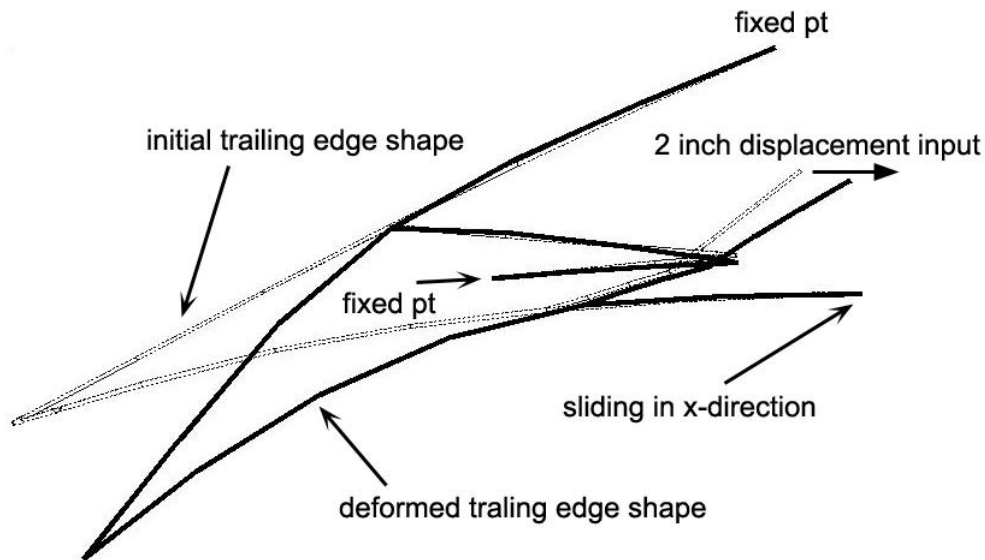


Figure 10: The trailing edge is required to deflect 10 degrees downwards. The horizontal dimension for his model is 35inch and the vertical dimension is 15inch. Maximum deflection is 6.121inch downwards at the tip of the trailing edge. The minimum and maximum in-plane beam dimensions are 0.052inch and 0.1174inch respectively, and the out-of-plane dimension is 1inch.

5. DISCUSSIONS

5.1. Number of design variables and design resolution

As opposed to using each finite element dimension as a topology variable, the path representation utilizes the intermediate connection ports to define the topology and shape. The dimensions, on the other hand, are determined by the sections along each path. Therefore, the number of design variables, including the connection ports and path section dimensions, are reduced and are independent of the resolution of the final design. This eliminates the need to pre-specify the solution resolution, which has typically been defined during the design domain discretization.

5.2. Convergence to local optimum

As seen in Figure 9 and Figure 10, the desired shape morphing can be achieved with the optimal compliant mechanism found from the GA. Although some minor errors can still be seen in the examples, we suspect that it is because the optimal design found from the approach is not exactly a local optimum. In fact, this is one of the drawbacks using GA. Due to its heuristic property, GA can efficiently search in a large solution space, while converging to a local optimum can be quite difficult. However, we believe the designs in Figure 9 and Figure 10 are very close to the local optima nearby. The shape deviation can be further reduced if a gradient-based local search is implemented following the GA or embedded within the GA.

5.3. Boundary conditions

It is observed that the locations of the fixed points are critical to the solution, because they provide points which the whole structure pivots about. In fact, the topology of a compliant mechanism not only includes the connectivity of the nodes, but it also includes the relative location of input, output, and fixed points, i.e. the boundary conditions. In this research, the locations of the fixed points are specified and fixed throughout the GA. The boundary conditions are changed only when the pTop of a path to or from a fixed point is set to zero. However, the locations of the fixed points can be further included into the shape design variables to study the effect of their locations.

5.4. Objective function

We previously developed two curve comparison schemes, using LSE and a modified Fourier Transformation (FT)¹⁰. However, all the examples shown in Figure 9 and Figure 10 are obtained using LSE deviation as the objective function.

Although the modified FT can give similar results and even the mirror images, its calculation time is longer than that required for LSE deviation. Therefore, we believe LSE deviation is sufficient for evaluating the shape morphing effectiveness.

6. SUMMARY

A synthesis approach using a load path representation method is presented in this paper to design shape morphing compliant mechanisms. The design variable data structure, using the path information, allows the GA to efficiently detect the invalid designs and exclude them from the solution space. The results demonstrate the capability of the load path representation method to create various designs with less design variables, compared to the element network discretization approach. The results also show that the use of compliant mechanisms can indeed achieve the desired shape morphing, thus providing a viable alternative for shape morphing. In order to improve the convergence to a local optimum, we are currently incorporating a local search within or following the GA. At the same time, we are constantly exploring new applications that can potentially benefit from shape morphing compliant mechanisms.

ACKNOWLEDGEMENT

Authors gratefully acknowledge the funding support of U.S. Air Force Office of Scientific Research for this work under the research contract number F49620-96-1-0205.

REFERENCE

1. Washington, G., Yoon, H.S., Angelino, M., and Theunissen, W.H., "Design, Modeling, and Optimization of Mechanically Reconfigurable Aperture Antennas," *IEEE Transactions on Antennas and Propagation*, **50**(5), pp.628-637, 2002.
2. Lawson, P.R. and Yen, J.L., "A Piecewise Deformable Subreflector for Compensation of Cassegrain Main Reflector Errors", *IEEE Transactions on Antennas and Propagation*, **36**(10):1343-1350, 1988.
3. Washington, G., "Smart Aperture Antennas", *Journal of Smart Materials and Structures*, **5**(6):801-805, 1996.
4. Martin, J.W., Main, J.A., and Nelson, G.C., "Shape Control of Deployable Membrane Mirrors", *ASME Adaptive Structures and Materials Systems Conference*, ad57/md83, pp.217-223, 1998.
5. Martin, J.W., Redmond, J.M., Barney, P.S., Henson, T.D., Wehlburg, J.C., and Main, J.A., "Distributed Sensing and Shape Control of Piezoelectric Bimorph Mirrors", *Journal of Intelligent Material Systems and Structures*, **11**, pp.744-757, 2000.
6. Yoon, H.S. and Washington, G., "Piezoceramic Actuated Aperture Antennae", *Journal of Smart Materials and Structures*, **7**(4):537-542, 1998.
7. Yoon, H.S., Washington, G., and Theunissen, W.H., "Analysis and Design of Doubly Curved Piezoelectric Strip-Actuated Aperture Antennas", *IEEE Transactions on Antennas and Propagation*, **48**(5):755-763, 2000.
8. Angelino, M. and Washington, G., "Point Actuated Aperture Antenna Development", *Proceedings of SPIE*, 4334, pp.147-155, 2001.
9. Lu, K.J. and Kota, S., "Compliant Mechanism Synthesis for Shape-Change Applications: Preliminary Results," *Proceedings of the 2002 SPIE Modeling, Signal Processing, and Control Conference*, 4693, pp.161-172, San Diego, CA, 2002.
10. Lu, K.J. and Kota, S., "Design of Compliant Mechanisms for Morphing Structural Shapes," *Journal of Intelligent Materials Systems and Structures*, 2003 (in review).
11. Bendsoe, M.P. and Kikuchi, N., "Generating Optimal Topologies in Structural Design Using a Homogenization Method," *Computer Methods in Applied Mechanics and Engineering*, **71**, pp.197-224, 1988.
12. Anathasuresh, G.K., Kota, S., and Kikuchi, N., "Strategies for Systematic Synthesis of Compliant MEMS", *ASME Winter Annual Meeting*, 55(2), pp.677-686, 1994.
13. Frecker, M.I., "Optimal Design of Compliant Mechanisms", Ph.D. thesis, University of Michigan, Ann Arbor, MI, USA, 1997.
14. Hetrick, J.A. and Kota, S., "An Energy Formulation for Parametric Size and Shape Optimization of Compliant Mechanisms", *Journal of Mechanical Design*, **121**, pp.229-234, 1999.

15. Joo, J., Kota, S., and Kikuchi, N., "Nonlinear Synthesis of Compliant Mechanisms: Topology Design", *Proceedings of 2000 ASME Design Engineering Technical Conferences*, DETC2000/MECH-14141, 2002.
16. Canfield, S., Edinger, B., Frecker, M., and Koopman, G., "Design of Piezoelectric Inchworm Actuator and Compliant End-Effector for Minimally Invasive Surgery," *Proceedings SPIE Smart Structures and Materials*, 3668, pp.835-843, Newport Beach, CA, 1999.
17. Saggere, L. and Kota, S., "Static Shape Control of Smart Structures Using Compliant Mechanisms," *AIAA*, **37**(5), pp.572-578, 1999.